
Cross-Model Disagreement as a Label-Free Correctness Signal

Matt Gorbett
Independent Researcher
matthewgorbett@gmail.com

Suman Jana
Department of Computer Science
Columbia University
New York, NY 10027, USA
sj2536@columbia.edu

Abstract

Detecting when a language model is wrong without ground truth labels is a fundamental challenge for safe deployment. Existing approaches rely on a model’s own uncertainty, such as token entropy or confidence scores, but these signals fail critically on the most dangerous failure mode: confident errors, where a model is wrong but certain. In this work we introduce *cross-model disagreement* as a correctness indicator — a simple, training-free signal that can be dropped into existing production systems, routing pipelines, and deployment monitoring infrastructure without modification. Given a model’s generated answer, cross-model disagreement computes how surprised or uncertain a second verifier model is when reading that answer via a single forward pass. No generation from the verifying model is required, and no correctness labels are needed. We instantiate this principle as **Cross-Model Perplexity (CMP)**, which measures the verifying model’s surprise at the generating model’s answer tokens, and **Cross-Model Entropy (CME)**, which measures the verifying model’s uncertainty at those positions. Both **CMP** and **CME** outperform within-model uncertainty baselines across benchmarks spanning reasoning, retrieval, and mathematical problem solving (MMLU, TriviaQA, and GSM8K). On MMLU, **CMP** achieves a mean AUROC of 0.75 against a within-model entropy baseline of 0.59. These results establish cross-model disagreement as a practical, training-free approach to label-free correctness estimation, with direct applications in deployment monitoring, model routing, selective prediction, data filtering, and scalable oversight of production language model systems.

1 Introduction

Language models fail in two distinct ways. The first is ignorance: the model does not know the answer and signals this through uncertainty. Token entropy, maximum softmax probability (Hendrycks & Gimpel, 2017), and related signals are reasonable proxies for this failure mode, and the routing literature has built effective systems around them (Ding et al., 2024; Ong et al., 2025). The second failure mode is harder: the model is wrong but certain. It produces a fluent, high-confidence answer that happens to be incorrect. Within-model uncertainty signals are blind to this case by construction, since a confident model has low entropy regardless of whether its answer is right (Guo et al., 2017). Yet this is precisely the failure mode that matters most in practice. A medical assistant confidently stating the wrong drug interaction, a legal summarizer confidently misreading a statute, a student model confidently propagating a misconception: these are the errors that cause harm, and existing signals give no warning.

The confident error problem is not merely a calibration issue. Even well-calibrated models (Srinivas et al., 2024) cannot detect their own errors through introspection: a model that is wrong has, by definition, already committed to a wrong answer. Any signal derived solely from the generating model’s own distribution is fundamentally limited. It can tell you how confident the model is, but not whether that confidence is warranted. What is needed is an external perspective: a second model that can evaluate the generating model’s answer and flag disagreement.

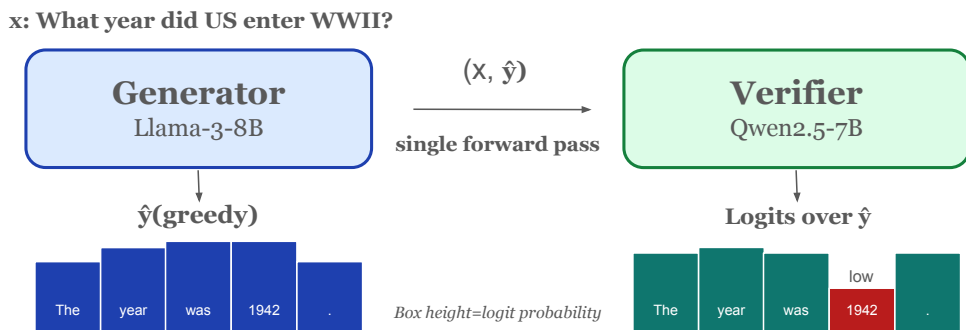


Figure 1: **Cross-model disagreement as a label-free correctness indicator.** Given a prompt x , the generator (Llama-3-8B) produces an answer \hat{y} . The verifier (Qwen2.5-7B) performs a single forward pass over (x, \hat{y}) with no generation required. The verifier assigns low probability to the token “1942”, the generator’s confident but incorrect answer. Cross-model perplexity (CMP) aggregates this surprise signal into a single correctness indicator, and high CMP flags a likely error.

This observation motivates *cross-model disagreement* as a practical signal. Rather than asking whether a model is uncertain about its own answer, we ask whether a second model is surprised by it. Concretely, given prompt x and generating model answer \hat{y} , we perform a single forward pass through a verifying model on (x, \hat{y}) and extract two signals: **CMP**, which aggregates the verifying model’s token-level surprise, and **CME**, which aggregates its token-level uncertainty. No generation from the verifier is required and no correctness labels are needed. The two signals are complementary: **CMP** is most effective when the generator is confidently wrong and the verifier assigns low probability to the specific incorrect tokens; **CME** is more informative on retrieval tasks where distributional uncertainty better reflects whether an answer is grounded. Across our evaluation, **CMP** outperforms within-model entropy on MMLU across 12 of 15 model pairs by AUROC, and **CME** leads on TriviaQA where distributional uncertainty is more informative than token-level surprise. When used as a routing signal—directing queries to the verifier only when disagreement is high—**CMP** recovers a substantial fraction of the performance gap between generator and verifier with no labels required, as measured by APGR (Ong et al., 2025). **CMP** wins 12 of 16 routing comparisons against within-model entropy on GSM8K, and achieves mean APGR of 0.915 on MMLU versus 0.848 for G-Ent.

The closest prior work uses cross-model consistency as a hallucination signal. SelfCheckGPT (Manakul et al., 2023) checks consistency across stochastic samples from the same model; CrossCheckGPT (Sun et al., 2024) compares outputs generated by multiple independent models. Both require multiple generations. Our setting is fundamentally different: we use a single greedy answer and a single forward pass through the verifier, with no generation from either model after the initial answer, and we target per-instance correctness prediction rather than hallucination ranking. More broadly, the uncertainty quantification literature has focused entirely on signals derived from the generating model itself (Kadavath et al., 2022; Kuhn et al., 2023; Liu et al., 2020), and prior work explicitly notes that within-model perplexity fails (Srinivas et al., 2024). To our knowledge, no prior work uses a verifying model’s logit-based signals on a generating model’s answer.

CMP and **CME** have direct applications in several settings. In *deployment monitoring*, **CMP** and **CME** can be evaluated on every query without ground truth labels, serving as a cheap triage signal that flags likely errors for more expensive downstream verification—whether human review, re-querying, or generation-based methods such as LLM-as-judge (Zheng et al., 2023). In *model routing*, high disagreement triggers escalation to a stronger model, recovering a large fraction of the performance gap at a fraction of the cost of always using the strong model. Unlike supervised routers such as RouteLLM (Ong et al., 2025), **CMP** and **CME** require no preference labels and no router training, occupying a different point on the supervision-cost tradeoff. In *data filtering*, high **CMP** on a candidate example identifies instances where models disagree—a label-free signal for hard or ambiguous examples useful for training data curation and hard negative mining. Finally, in *selective prediction* (Geifman

& El-Yaniv, 2017), high **CMP** serves as an abstention signal, allowing a system to withhold predictions on inputs where confident errors are most likely — improving accuracy on the subset it does answer without any labeled data or threshold calibration.

We further characterize when cross-model signals are most effective: on MMLU, **CMP** AUROC is uncorrelated with capability gap ($\rho = 0.11$, $p = 0.72$), suggesting architectural diversity drives correctness detection rather than capability asymmetry; on TriviaQA, **CME** is more robust across gap sizes; on GSM8K both signals improve modestly but without a significant trend. We discuss implications for scalable oversight and deployment monitoring in Section 5.

Our contributions are as follows:

- We introduce *cross-model disagreement* as a label-free, training-free correctness indicator, instantiated as **CMP** and **CME**, each requiring only a single forward pass through a verifying model with no generation, no correctness labels, and no router training.
- We show that **CMP** and **CME** outperform within-model uncertainty baselines across MMLU, TriviaQA, and GSM8K, and characterize when each signal is most effective depending on the nature of the failure mode.
- We show that on knowledge-intensive tasks, architectural diversity between same-sized models is sufficient for effective correctness detection, and capability asymmetry is not required, while on open-ended retrieval a stronger verifier provides meaningful additional benefit.

2 Related Work

Our work sits at the intersection of several research areas: LLM uncertainty estimation, model routing, LLM-as-Judge, scalable oversight, ensemble methods, and speculative decoding. We review each, clarifying how cross-model disagreement relates to and differs from prior work.

Uncertainty Estimation. A standard approach to predicting model correctness is to use the model’s own confidence as a proxy. Maximum softmax probability (Hendrycks & Gimpel, 2017) and predictive entropy are common baselines, but modern networks are poorly calibrated (Guo et al., 2017) and frequently assign high confidence to incorrect predictions. Srinivas et al. (2024) show explicitly that within-model perplexity has limited predictive power in open-ended settings. Self-evaluation (Kadavath et al., 2022), semantic consistency (Kuhn et al., 2023), and cross-model consistency (Manakul et al., 2023; Sun et al., 2024) improve on this but require multiple generation passes. **CMP** and **CME** require a single verifier forward pass and remain informative precisely where within-model entropy is flat.

LLM Routing. Routing systems reduce inference cost by directing queries to a stronger model only when needed. HybridLLM (Ding et al., 2024), RouteLLM (Ong et al., 2025), and FrugalGPT (Chen et al., 2023b) train routers on labeled preference data or correctness supervision; AutoMix (Aggarwal et al., 2024) uses a smaller model to self-verify before escalating but still requires a calibration step. All depend on task-specific labels. **CMP** and **CME** are parameter-free and require no router training, although they do require a single forward pass through a second model at inference time. We adopt the APGR metric from Ong et al. (2025) to measure routing quality in our experiments.

Ensemble Methods. Ensemble methods reduce prediction uncertainty by aggregating disagreement across multiple independently trained models (Lakshminarayanan et al., 2017). Cross-model disagreement shares this intuition but is asymmetric: the verifier responds to the generator’s specific answer rather than contributing a symmetric vote. This makes **CMP** and **CME** directional correctness signals rather than general uncertainty measures, and requires no task-specific training or ensemble construction.

LLM-as-Judge. A growing body of work uses a stronger language model to evaluate the outputs of a weaker one (Zheng et al., 2023; Dubois et al., 2024; Kim et al., 2024). These approaches target output quality and preference rather than per-instance correctness prediction, and all require generation from the judge—typically a full response or structured

critique. Our verifier performs only a single forward pass with no generation, producing a scalar correctness signal rather than natural language feedback.

Scalable Oversight. Scalable oversight (Bowman et al., 2022) and weak-to-strong generalization (Burns et al., 2024) study how to supervise AI systems whose capabilities may exceed those of the overseer, generally assuming that effective verification requires a more capable model. We examine whether capability gap is necessary or whether architectural diversity alone is sufficient, evaluating pairs with similar task accuracy alongside asymmetric ones.

Speculative Decoding. Speculative decoding (Leviathan et al., 2023; Chen et al., 2023a) accelerates inference by using a small draft model to propose tokens, which a larger target model verifies via acceptance sampling. **CMP** is the sequence-level analogue: rather than per-token accept/reject decisions, we aggregate verifier log-probabilities across the full answer into a single routing score. This connection grounds why **CMP** is most effective on tasks where errors manifest as low token-level acceptance probability.

3 Method

In this section we describe cross-model disagreement. Given a *generating model* \mathcal{M}_g and a *verifying model* \mathcal{M}_v , we define two label-free signals for predicting whether \mathcal{M}_g 's answer is correct.

Problem Setup. Let x denote an input prompt. The generating model produces an answer $\hat{y}_g \sim \mathcal{M}_g(\cdot | x)$ autoregressively via greedy decoding. Our goal is to predict whether \hat{y}_g is correct without access to ground truth labels. We make no assumptions about the relative capability of \mathcal{M}_g and \mathcal{M}_v .

3.1 Cross-Model Perplexity

Given \hat{y}_g , we concatenate the prompt and answer to form (x, \hat{y}_g) and perform a single forward pass through \mathcal{M}_v . At each answer token position $t \in \{1, \dots, T\}$, the forward pass yields logits over the full vocabulary. We define **CMP** as:

$$\text{CMP}(x, \hat{y}_g) = \exp \left(-\frac{1}{T} \sum_{t=1}^T \log p_v \left(\hat{y}_g^{(t)} \mid x, \hat{y}_g^{(<t)} \right) \right) \quad (1)$$

where p_v denotes the verifying model's conditional distribution and T is the number of answer tokens. High **CMP** indicates that \mathcal{M}_v assigns low probability to \mathcal{M}_g 's answer—the models disagree. **CMP** connects formally to speculative decoding (Leviathan et al., 2023; Chen et al., 2023a), where the acceptance probability for a draft token x_t is $\min(1, p_v(x_t)/p_g(x_t))$. **CMP** aggregates this token-level acceptance signal across the full answer sequence, making a single binary decision rather than a token-level correction.

3.2 Cross-Model Entropy

From the same single forward pass, we also compute **CME** as the mean entropy of the verifying model's output distribution over answer token positions:

$$\text{CME}(x, \hat{y}_g) = -\frac{1}{T} \sum_{t=1}^T \sum_v p_v(v \mid x, \hat{y}_g^{(<t)}) \log p_v(v \mid x, \hat{y}_g^{(<t)}) \quad (2)$$

Where **CMP** measures the verifying model's surprise at the specific tokens produced, **CME** measures its general uncertainty at those positions. The two signals are complementary: **CMP** is most informative when the generator is confidently wrong and the verifier assigns low probability to the specific incorrect tokens; **CME** is most informative on retrieval tasks where the verifier's distributional uncertainty better reflects whether the answer is grounded. Both signals are obtained at no additional computational cost beyond the single forward pass required for **CMP**.

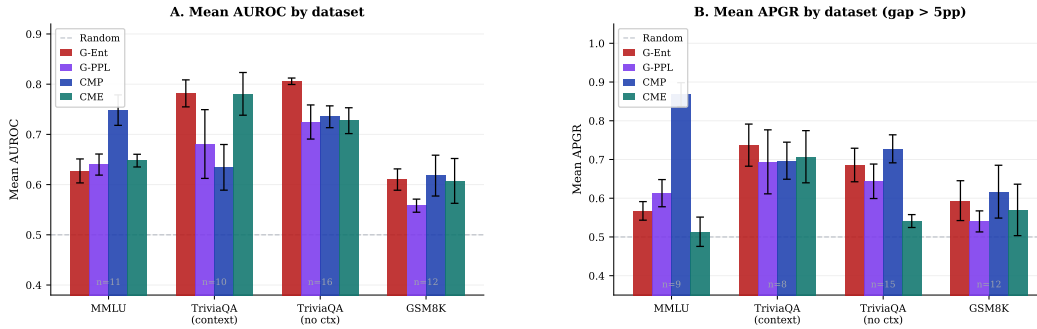


Figure 2: **CMP** and **CME** performance across datasets compared to baselines. (A) Mean AUROC over all model pairs. G-Ent and G-PPL measure the generator’s own entropy and perplexity; CME and CMP measure the corresponding signals from a verifier model on the generator’s answer. APGR measures the fraction of the performance gap between weak and strong model that is recovered by routing, normalized so that random routing scores 0 and oracle routing scores 1; pairs with small gaps are excluded because the small denominator in the PGR formula produces unstable estimates. Error bars show standard error across pairs; n indicates the number of pairs per dataset.

4 Experiments

We evaluate **CMP** and **CME** across four benchmarks datasets. Table 1 summarizes selected results; full results appear in Appendix A.

Datasets. We evaluate on MMLU (Hendrycks et al., 2021) (multiple-choice), TriviaQA (Joshi et al., 2017) (with and without context), and GSM8K (Cobbe et al., 2021) (chain-of-thought reasoning), covering knowledge retrieval, reading comprehension, and multi-step arithmetic.

Models. We evaluate seven instruction-tuned models spanning five families: Qwen2.5 (0.5B, 7B), Llama-3 (1B, 8B), Gemma-3 (270M), Mistral (7B), and OLMo-3 (7B). We construct ordered model pairs across four datasets, covering both *asymmetric* pairs (small generator verified by large model, e.g. Qwen-0.5B \rightarrow Qwen-7B) and *same-sized cross-family* pairs among the four 7–8B models (Qwen-7B, Llama-3-8B, Mistral-7B, OLMo-7B), which isolate architectural diversity from capability asymmetry. Full model details and per-pair results are in Appendix C.

Baselines and metrics. We compare **CMP** and **CME** against two within-model baselines: *generator entropy* (G-Ent), the mean token-level entropy $H = -\sum_v p_v \log p_v$ over the generator’s answer tokens, and *generator perplexity* (G-PPL), the mean token-level perplexity of the generator on its own answer. Both are standard unsupervised signals requiring no verifier. Together these serve as direct ablations of **CME** and **CMP** respectively: if the cross-model signals merely recover information already present in the generator’s own distribution, G-Ent and G-PPL should perform comparably. We additionally test explicit verification prompting (P(True); Kadavath et al., 2022) on GSM8K, where the verifier is asked directly whether the generator’s answer is correct (Appendix F). We also compare against RouteLLM (Ong et al., 2025), the strongest supervised routing baseline, which trains a router on human preference labels augmented with LLM-judge data; unlike our signals, it requires labeled data and a trained router model, and we treat it as an upper bound on what supervision buys in this setting.

For correctness prediction we report AUROC against weak model incorrectness, which is threshold-free, requires no routing setup, and is our primary metric for evaluating signal quality across all pairs. For routing quality we report APGR (Average Performance Gap Recovered) (Ong et al., 2025). At each routing threshold, a fraction c of queries are sent to the strong model while the rest use the weak model’s answer, yielding accuracy $a(c)$. The performance gap recovered at cost c is:

$$\text{PGR}(c) = \frac{a(c) - a_w}{a_s - a_w}, \quad (3)$$

Table 1: Selected results across all four benchmarks. **Bold** = best per row among G-Ent, G-PPL, CMP, CME. Same-size cross-family pairs marked †. See Appendix for full results.

| Dataset | Generator | Verifier | Acc _g | Acc _v | Acc. Gap | AUROC ↑ | | | | APGR ↑ | | | |
|----------------------|-------------|------------|------------------|------------------|----------|--------------|--------------|--------------|--------------|--------------|--------------|--------------|--------------|
| | | | | | | G-Ent | G-PPL | CMP | CME | G-Ent | G-PPL | CMP | CME |
| MMLU | Qwen-0.5B | Qwen-7B | 0.42 | 0.72 | 0.30 | 0.591 | 0.557 | 0.842 | 0.587 | 0.522 | 0.502 | 0.789 | 0.500 |
| | Llama-1B | Llama-3-8B | 0.43 | 0.62 | 0.18 | 0.656 | 0.655 | 0.815 | 0.679 | 0.563 | 0.603 | 0.871 | 0.542 |
| | Llama-1B | Qwen-7B | 0.43 | 0.72 | 0.29 | 0.656 | 0.655 | 0.786 | 0.638 | 0.571 | 0.595 | 0.803 | 0.565 |
| | OLMo-7B† | Qwen-7B | 0.56 | 0.72 | 0.16 | 0.503 | 0.599 | 0.895 | 0.695 | 0.485 | 0.544 | 0.909 | 0.452 |
| | Mistral-7B† | Llama-3-8B | 0.56 | 0.62 | 0.06 | 0.720 | 0.725 | 0.753 | 0.717 | 0.712 | 0.855 | 0.956 | 0.623 |
| | Llama-3-8B† | Qwen-7B | 0.62 | 0.72 | 0.10 | 0.652 | 0.685 | 0.694 | 0.633 | 0.618 | 0.655 | 0.899 | 0.600 |
| TriviaQA | Llama-3-8B | Mistral-7B | 0.43 | 0.64 | 0.20 | 0.858 | 0.887 | 0.833 | 0.923 | 0.818 | 0.838 | 0.858 | 0.785 |
| | Qwen-0.5B | Qwen-7B | 0.41 | 0.65 | 0.24 | 0.773 | 0.726 | 0.818 | 0.824 | 0.619 | 0.598 | 0.737 | 0.606 |
| | Llama-1B | Qwen-7B | 0.54 | 0.65 | 0.10 | 0.805 | 0.811 | 0.691 | 0.788 | 0.696 | 0.724 | 0.764 | 0.574 |
| | Llama-3-8B† | Qwen-7B | 0.43 | 0.65 | 0.21 | 0.858 | 0.887 | 0.777 | 0.875 | 0.789 | 0.812 | 0.806 | 0.755 |
| | Mistral-7B† | Qwen-7B | 0.64 | 0.65 | 0.01 | 0.848 | 0.300 | 0.420 | 0.766 | 2.222 | -1.068 | -0.562 | 0.093 |
| | Llama-1B | Llama-3-8B | 0.42 | 0.67 | 0.25 | 0.840 | 0.851 | 0.938 | 0.813 | 0.687 | 0.694 | 0.813 | 0.588 |
| TriviaQA (no ctx) | Qwen-0.5B | Qwen-7B | 0.21 | 0.59 | 0.38 | 0.791 | 0.786 | 0.799 | 0.827 | 0.533 | 0.536 | 0.645 | 0.514 |
| | Llama-1B | Qwen-7B | 0.42 | 0.59 | 0.17 | 0.840 | 0.851 | 0.738 | 0.806 | 0.655 | 0.675 | 0.758 | 0.506 |
| | Qwen-7B† | Llama-3-8B | 0.59 | 0.67 | 0.08 | 0.823 | 0.794 | 0.752 | 0.634 | 0.993 | 0.953 | 0.976 | 0.564 |
| GSM8K | Mistral-7B† | Llama-3-8B | 0.51 | 0.61 | 0.11 | 0.655 | 0.539 | 0.719 | 0.687 | 0.872 | 0.638 | 0.998 | 0.887 |
| | Llama-1B | Qwen-7B | 0.38 | 0.90 | 0.51 | 0.543 | 0.523 | 0.668 | 0.666 | 0.511 | 0.503 | 0.574 | 0.562 |
| | Llama-1B | Llama-3-8B | 0.38 | 0.61 | 0.23 | 0.543 | 0.523 | 0.655 | 0.606 | 0.521 | 0.505 | 0.662 | 0.585 |
| | Qwen-0.5B | Qwen-7B | 0.25 | 0.90 | 0.64 | 0.616 | 0.621 | 0.629 | 0.682 | 0.520 | 0.521 | 0.528 | 0.539 |
| | OLMo-7B† | Qwen-7B | 0.83 | 0.90 | 0.07 | 0.763 | 0.538 | 0.748 | 0.808 | 0.960 | 0.657 | 0.956 | 0.950 |
| | Llama-3-8B† | Qwen-7B | 0.61 | 0.90 | 0.28 | 0.596 | 0.577 | 0.590 | 0.480 | 0.551 | 0.538 | 0.614 | 0.456 |

where a_w and a_s are the weak and strong model accuracies. APGR averages PGR over $c \in (0, 1)$: a value of 0 corresponds to random routing and 1 to oracle routing. Small accuracy gaps produce unstable APGR estimates due to the small denominator in $PGR(c)$; we therefore exclude such pairs from Figure 2.

4.1 Results

We evaluate **CMP** and **CME** against within-model baselines across four benchmarks and model pairs spanning asymmetric and same-sized cross-family configurations. Table 1 and Figure 2 summarize the main results: **CMP** leads on MMLU and GSM8K while **CME** is more competitive on TriviaQA, and both cross-model signals consistently outperform their within-model counterparts on tasks where the generator makes confident errors. The paragraphs below analyze the per-case signal structure, quintile separation, and conditions under which cross-model signals succeed or fail.

CMP targets the failure mode G-Ent misses. Figure 3 isolates the four outcome categories. On MMLU (OLMo-7B → Llama-8B), **CMP** in the “generator wrong only” case is $155\times$ the both-correct baseline—a $9\times$ spike over the remaining cases—while G-Ent is flat across all four ($\leq 1.0\times$ variation). On TriviaQA (Llama-8B → Qwen-7B) the pattern sharpens: **CMP** reaches 834k versus 97 when both models are correct ($10\times$ selectivity), while G-Ent rises by only $1.6\times$. G-Ent is elevated whenever the generator is uncertain regardless of whether the verifier concurs; **CMP** selectively spikes only when the generator’s error is not shared by the verifier.

Figure 2A reports mean AUROC across all model pairs. On MMLU, **CMP** achieves 0.797 versus 0.630 for G-Ent and 0.646 for G-PPL, leading in all six pairs. On GSM8K, **CMP** (0.668) and **CME** (0.655) both outperform G-Ent (0.619) and G-PPL (0.553), with G-PPL performing worst of all four signals—consistent with the near-flat quintile spread in Figure 3. On TriviaQA (context), **CME** leads (0.835) with G-Ent close behind (0.828), while **CMP** underperforms on several pairs where the verifier shares similar knowledge gaps to the generator. On TriviaQA (no context) the signals cluster tightly (G-Ent 0.824, G-PPL 0.821, **CMP** 0.807, **CME** 0.770) with no clear winner, consistent with retrieval errors being detectable by within-model signals when context is absent.

Task-dependent boundaries. On GSM8K, **CMP** achieves mean APGR of 0.589 versus 0.566 for G-Ent and wins 12 of 16 routing comparisons, but the per-case spike is weaker than on MMLU or TriviaQA, and **CME** is preferable on several pairs (Table 1). The Mistral-7B →

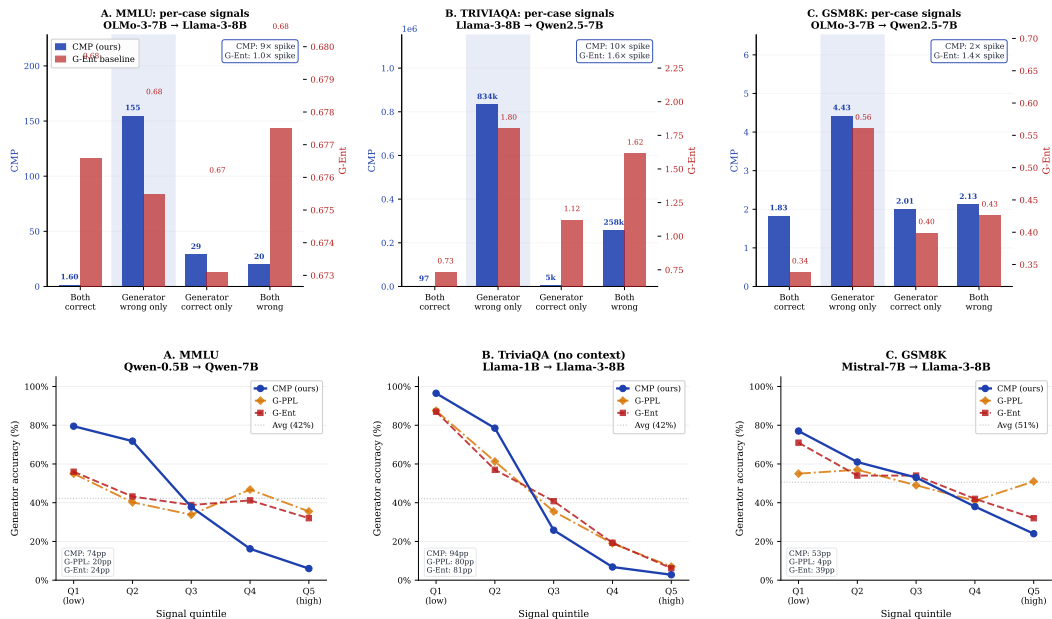


Figure 3: **Top row: per-case signal means.** Mean **CMP** (left axis, blue) and **G-Ent** (right axis, red) by outcome category. The shaded column highlights the “generator wrong only” case—confident errors the verifier does not share. On MMLU, **CMP** spikes 9× above the mean of the other three cases while **G-Ent** is flat (1.0×); on TriviaQA the spike is 10× vs. 1.6×; on GSM8K both signals rise modestly (2× and 1.4×), reflecting the difficulty of isolating chain-of-thought errors with token-level signals. **Bottom row: accuracy by signal quintile.** Samples sorted by signal strength (Q1 = lowest, Q5 = highest); bars show weak model accuracy within each bin. On MMLU, **CMP** produces a 74pp spread versus 24pp for **G-Ent** and 20pp for **G-PPL**. On TriviaQA (no context), all three signals are competitive (94pp, 81pp, 80pp). On GSM8K, **CMP** achieves a 53pp spread while **G-PPL** nearly collapses to 4pp, confirming that generator self-perplexity is uninformative on chain-of-thought tasks and that cross-model disagreement is doing genuine work.

Qwen-7B pair on TriviaQA is a more extreme case: with only a 1pp accuracy gap, **CMP** and **G-PPL** collapse near chance (AUROC 0.42 and 0.30) while **G-Ent** remains strong (0.848). Both cases point to the same boundary condition: when the verifier shares the generator’s failure mode—either through similar knowledge gaps or nearly identical accuracy—cross-model disagreement loses its signal, and within-model entropy is the more reliable fallback.

Final-answer tokens vs. full chain-of-thought. On GSM8K, we test whether **CMP**’s signal comes from the full chain-of-thought or only the final numerical answer. **CMP** restricted to answer tokens only (**CMP-Final**) achieves mean APGR of 0.665 versus 0.682 for the full trace (**CMP-Full**), indicating that the final answer carries most of the signal with a small additional benefit from the reasoning steps. This suggests **CMP** could be applied more efficiently by scoring only the answer tokens, avoiding the cost of processing the full chain-of-thought through the verifier.

Implicit perplexity vs. explicit verification prompting. We test $P(\text{True})$ (Kadavath et al., 2022): prompting the verifier with “Is the proposed answer correct?” and extracting the probability of Yes. $P(\text{True})$ achieves mean APGR of only 0.492 (random) confirming that implicit token-level perplexity far outperforms explicit correctness judgments. This is consistent with known limitations of LLM self-evaluation on mathematical reasoning: models that cannot reliably solve a problem also cannot reliably judge whether a proposed solution is correct when asked directly. Full per-pair results in Appendix F.

Comparison to supervised routing. RouteLLM (Ong et al., 2025) provides the nearest supervised baseline: a causal LLM classifier trained on tens of thousands of human preference labels from Chatbot Arena, augmented with LLM-judge synthetic labels, routing between GPT-4 and Mixtral-8x7B. Their best augmented router achieves APGR of 0.622 on GSM8K

and 0.603 on MMLU. **CMP** achieves mean APGR of 0.682 on GSM8K and 0.915 on MMLU with zero labeled data and no router training. These evaluations are not directly comparable: RouteLLM routes between a proprietary strong model and an open-weight weak model across a different task and label distribution, while we route between open-weight pairs on standard benchmarks. We include the comparison not as a controlled benchmark but to situate **CMP** on the broader supervision-cost tradeoff: a single verifier prefill with no labeled data is competitive with a trained supervised router on reasoning tasks, and the gap is substantial on knowledge-intensive multiple-choice. Where labeled routing data can be collected, supervised routers remain the appropriate choice.

5 Discussion

5.1 Routing performance and compute tradeoffs

Figure 2B reports mean APGR across pairs with accuracy gap $> 5\text{pp}$. **CMP** leads on MMLU and GSM8K; on TriviaQA, G-Ent and **CME** are competitive, consistent with the AUROC results.

The practical regime where **CMP** is most attractive is one where generation cost dominates and no labeled routing data is available. Routing with **CMP** or **CME** requires a single verifier prefill on every query, with no autoregressive generation from the verifier and no router model. On MMLU this prefill is negligible; on GSM8K, where chain-of-thought traces reach up to 256 tokens, it is more substantial but still well below the cost of strong-model generation. Critically, the prefill is incurred only to make a routing decision: queries correctly identified as easy are served by the weak model with no further large-model compute. If the verifier generated rather than prefilled, verifier compute would be incurred on every query regardless of the routing outcome, largely eliminating the cost benefit. Prefill-only is therefore what makes label-free routing economically viable on long-form tasks, not a concession.

Existing approaches occupy different points on this tradeoff. Label-based routers such as RouteLLM (Ong et al., 2025) and HybridLLM (Ding et al., 2024) add negligible inference overhead but require labeled preference data and a trained router model. FrugalGPT (Chen et al., 2023b) and AutoMix (Aggarwal et al., 2024) avoid large-model compute on easy queries entirely but require calibration steps or supervised signals. **CMP** and **CME** occupy the opposite corner: zero labeled data, zero router training, one verifier prefill per query. The tradeoff is explicit: where labeled routing data can be collected, supervised routers remain the appropriate choice; **CMP** and **CME** are most valuable precisely when such data is unavailable.

5.2 When Does Capability Gap Matter?

Figure 4 plots **CMP** AUROC against accuracy gap for all pairs across three benchmarks. The task-dependent pattern is stark. On MMLU, **CMP** is essentially uncorrelated with capability gap ($\rho = +0.11$, $p = 0.72$): pairs with a 6-point accuracy gap perform as well as pairs with a 47-point gap, and the highest-scoring points are same-size cross-family pairs (blue), not the largest-gap pairs. The operative mechanism on knowledge-intensive multiple-choice tasks appears to be diversity of training rather than capability asymmetry—models from different families make different confident errors, and **CMP** captures this disagreement regardless of relative accuracy.

On TriviaQA the picture is different. **CMP** shows a significant positive correlation with capability gap ($\rho = +0.60$, $p = 0.04$), with large-gap pairs substantially outperforming small-gap pairs (AUROC 0.78 vs. 0.59). Open-ended knowledge retrieval requires the verifier to have genuine knowledge the generator lacks; a same-sized peer from a different family may share the same knowledge gaps, reducing the informativeness of its surprise. The two same-size cross-family pairs on TriviaQA (blue) sit at the lower end of the performance range, consistent with this interpretation. **CME** is more robust to this effect, remaining competitive across gap sizes.

On GSM8K there is no significant trend ($\rho = -0.11$, $p = 0.40$), with high variance across pairs at similar gap sizes. Signal quality on chain-of-thought tasks appears driven more by

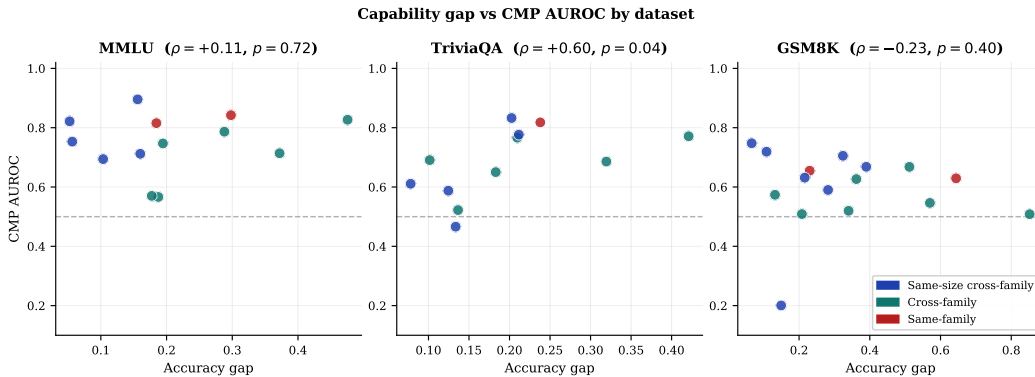


Figure 4: **CMP** AUROC versus capability gap across three benchmarks. On MMLU, AUROC is uncorrelated with gap ($\rho = +0.11$, $p = 0.72$) and same-size cross-family pairs (blue) achieve the highest scores, suggesting model diversity drives the signal rather than capability asymmetry. On TriviaQA, gap correlates positively with AUROC ($\rho = +0.60$, $p = 0.04$), indicating a stronger verifier helps when errors are knowledge-driven. GSM8K shows no significant trend ($\rho = -0.11$, $p = 0.40$).

model family and architectural diversity than by capability gap, though the modest overall AUROC levels make these patterns harder to interpret cleanly.

5.3 Implications for Scalable Oversight

The scalable oversight literature (Bowman et al., 2022; Burns et al., 2024) has largely assumed that verifying a model’s outputs requires a more capable supervisor. Our results qualify this assumption in a task-dependent way. On MMLU, peer verification between same-sized models of different families is as effective as verification by a substantially stronger model, suggesting that for knowledge-intensive tasks the capability hierarchy is not a prerequisite for correctness detection — architectural diversity is sufficient. On open-ended retrieval tasks, a stronger verifier does provide meaningful benefit, consistent with the intuition that the verifier needs knowledge the generator lacks.

The practical implication is straightforward: the right verification strategy depends on the likely failure mode of the deployed model. For knowledge-intensive tasks with constrained output formats, a diverse peer model is a sufficient and efficient verifier. For open-ended retrieval, a stronger verifier improves detection quality. This task-dependent characterization is a concrete and actionable finding for deployment monitoring without labeled data.

6 Conclusion

We have shown that cross-model disagreement—measured as **CMP** or **CME** via a single forward pass through a verifying model—is a reliable label-free correctness signal for language model outputs. The signal is strongest when errors are confident rather than ignorance-based, works between same-sized models of different families, and requires no labeled data or router training.

Several directions remain open. First, we evaluate on greedy-decoded answers; extending cross-model disagreement to sampled or chain-of-thought outputs, where the generating model’s answer is not a single deterministic sequence, is a natural next step. Second, our results characterize which signal works for which failure mode empirically, but a theoretical account of this dependence would deepen the understanding. Third, we evaluate on classification and short-form generation; applying cross-model disagreement to long-form generation, code, and multi-step reasoning at scale would test the limits of the framework. Fourth, the diversity mechanism we identify raises a concrete design question: given a fixed verifier budget, how should one select a verifying model to maximize correctness signal? Representational similarity metrics may provide a principled answer. Finally, our scalable oversight results are at inference time on static benchmarks; whether peer verification can support iterative oversight loops as both models scale is the central open question that connects this work to the broader alignment agenda.

References

- Pranjal Aggarwal, Aman Madaan, Yiming Yang, and Mausam. AutoMix: Automatically mixing language models. In *Findings of the Association for Computational Linguistics: EMNLP 2024*, 2024.
- Samuel R Bowman, Jeeyoon Hyun, Ethan Perez, Edwin Chen, Craig Pettit, Scott Heiner, Kamilė Lukošiuūtė, Amanda Askell, Andy Jones, Anna Chen, et al. Measuring progress on scalable oversight for large language models. *arXiv preprint arXiv:2211.03540*, 2022.
- Collin Burns, Pavel Izmailov, Jan Hendrik Kirchner, Bowen Baker, Leo Gao, Leopold Aschenbrenner, Yining Chen, Adrien Ecoffet, Manas Joglekar, Jan Leike, Ilya Sutskever, and Jeff Wu. Weak-to-strong generalization: Eliciting strong capabilities with weak supervision. In *International Conference on Machine Learning*. PMLR, 2024.
- Charlie Chen, Sebastian Borgeaud, Geoffrey Irving, Jean-Baptiste Lespiau, Laurent Sifre, and John Jumper. Accelerating large language model decoding with speculative sampling. *arXiv preprint arXiv:2302.01318*, 2023a.
- Lingjiao Chen, Matei Zaharia, and James Zou. Frugalgpt: How to use large language models while reducing cost and improving performance, 2023b. URL <https://arxiv.org/abs/2305.05176>.
- Karl Cobbe, Vineet Kosaraju, Mohammad Bavarian, Mark Chen, Heewoo Jun, Lukasz Kaiser, Matthias Plappert, Jerry Tworek, Jacob Hilton, Reiichiro Nakano, et al. Training verifiers to solve math word problems. In *arXiv preprint arXiv:2110.14168*, 2021.
- Dujian Ding, Ankur Mallick, Chi Wang, Robert Sim, Subhabrata Mukherjee, Victor Ruhle, Laks VS Lakshmanan, and Ahmed Hassan Awadallah. Hybrid LLM: Cost-efficient and quality-aware query routing. In *International Conference on Learning Representations*, 2024.
- Yann Dubois, Chen Xuechen Li, Rohan Taori, Tianyi Zhang, Ishaan Gulrajani, Jimmy Ba, Carlos Guestrin, Percy S Liang, and Tatsunori B Hashimoto. AlpacaFarm: A simulation framework for methods that learn from human feedback. In *Advances in Neural Information Processing Systems*, volume 36, 2024.
- Yonatan Geifman and Ran El-Yaniv. Selective classification for deep neural networks. In *Advances in Neural Information Processing Systems*, volume 30, 2017.
- Chuan Guo, Geoff Pleiss, Yu Sun, and Kilian Q Weinberger. On calibration of modern neural networks. In *International Conference on Machine Learning*, pp. 1321–1330. PMLR, 2017.
- Dan Hendrycks and Kevin Gimpel. A baseline for detecting misclassified and out-of-distribution examples in neural networks. In *International Conference on Learning Representations*, 2017.
- Dan Hendrycks, Collin Burns, Steven Basart, Andy Zou, Mantas Mazeika, Dawn Song, and Jacob Steinhardt. Measuring massive multitask language understanding. In *International Conference on Learning Representations*, 2021.
- Mandar Joshi, Eunsol Choi, Daniel S Weld, and Luke Zettlemoyer. TriviaQA: A reading comprehension dataset containing trivia questions. *arXiv preprint arXiv:1705.03551*, 2017.
- Saurav Kadavath, Tom Conerly, Amanda Askell, Tom Henighan, Dawn Drain, Ethan Perez, Nicholas Schiefer, Zac Hatfield-Dodds, Nova DasSarma, Eli Tran-Johnson, et al. Language models (mostly) know what they know. In *arXiv preprint arXiv:2207.05221*, 2022.
- Seungone Kim, Jamin Shin, Yejin Cho, Joel Han, Shayne Longpre, Hwaran Moon, Sangdoon Yun, Seongjin Shin, Sungdong Kim, James Thorne, et al. Prometheus: Inducing fine-grained evaluation capability in language models. In *The Twelfth International Conference on Learning Representations*, 2024.
- Lorenz Kuhn, Yarin Gal, and Sebastian Farquhar. Semantic uncertainty: Linguistic invariances for uncertainty estimation in natural language generation. In *International Conference on Learning Representations*, 2023.

-
- Balaji Lakshminarayanan, Alexander Pritzel, and Charles Blundell. Simple and scalable predictive uncertainty estimation using deep ensembles. In *Advances in Neural Information Processing Systems*, 2017.
- Yaniv Leviathan, Matan Kalman, and Yossi Matias. Fast inference from transformers via speculative decoding. In *International Conference on Machine Learning*, pp. 19274–19286. PMLR, 2023.
- Weitang Liu, Xiaoyun Wang, John Owens, and Yixuan Li. Energy-based out-of-distribution detection. In *Advances in Neural Information Processing Systems*, volume 33, pp. 21464–21475, 2020.
- Potsawee Manakul, Adian Liusie, and Mark JF Gales. Selfcheckgpt: Zero-resource black-box hallucination detection for generative large language models. In *Proceedings of the 2023 Conference on Empirical Methods in Natural Language Processing*, pp. 9004–9017, 2023.
- Isaac Ong, Amjad Almahairi, Vincent Wu, Wei-Lin Chiang, Tianhao Wu, Joseph E Gonzalez, M Waleed Kadous, and Ion Stoica. RouteLLM: Learning to route LLMs with preference data. In *International Conference on Learning Representations*, 2025.
- Nikhil Srinivas, Mohammed Shoaib, and Himabindu Lakkaraju. Large language models must be taught to know what they don’t know. In *Advances in Neural Information Processing Systems*, 2024.
- Guangzhi Sun, Potsawee Manakul, Adian Liusie, Kunat Pipatanakul, Chao Zhang, Phil Woodland, and Mark Gales. Crosscheckgpt: Universal hallucination ranking for multi-modal foundation models. *arXiv preprint arXiv:2405.13684*, 2024.
- Lianmin Zheng, Wei-Lin Chiang, Ying Sheng, Siyuan Zhuang, Zhanghao Wu, Yonghao Zhuang, Zi Lin, Zhuohan Li, Dacheng Li, Eric Xing, et al. Judging LLM-as-a-judge with MT-bench and chatbot arena. In *Advances in Neural Information Processing Systems*, volume 36, 2023.

Appendix

A Full Results

Tables 2–5 report per-pair results across all four benchmarks. Pairs are grouped by type—same-size cross-family, cross-family asymmetric, and same-family asymmetric—and sorted by capability gap (descending) within each group. For each pair we report AUROC and APGR for the within-model entropy baseline (G-Ent), within-model perplexity (G-PPL), cross-model perplexity (CMP), and cross-model entropy (CME). Bold indicates the best signal per row.

Table 2: Full results on MMLU. Pairs grouped by type and sorted by capability gap (descending). **Bold** = best per row among G-Ent, G-PPL, CMP, CME.

| Generator | Verifier | Acc _g | Acc _v | Gap | AUROC ↑ | | | | APGR ↑ | | | |
|--------------------------------|------------|------------------|------------------|------|---------|--------------|--------------|--------------|--------|--------------|--------------|-------|
| | | | | | G-Ent | G-PPL | CMP | CME | G-Ent | G-PPL | CMP | CME |
| <i>Same-size cross-family</i> | | | | | | | | | | | | |
| Mistral-7B | Qwen-7B | 0.56 | 0.72 | 0.16 | 0.720 | 0.725 | 0.712 | 0.633 | 0.607 | 0.659 | 0.808 | 0.606 |
| OLMo-7B | Qwen-7B | 0.56 | 0.72 | 0.16 | 0.503 | 0.599 | 0.895 | 0.695 | 0.485 | 0.544 | 0.909 | 0.452 |
| Llama-3-8B | Qwen-7B | 0.62 | 0.72 | 0.10 | 0.652 | 0.685 | 0.694 | 0.633 | 0.618 | 0.655 | 0.899 | 0.600 |
| Mistral-7B | Llama-3-8B | 0.56 | 0.62 | 0.06 | 0.720 | 0.725 | 0.753 | 0.717 | 0.712 | 0.855 | 0.956 | 0.623 |
| OLMo-7B | Llama-3-8B | 0.56 | 0.62 | 0.05 | 0.503 | 0.599 | 0.822 | 0.690 | 0.485 | 0.581 | 1.033 | 0.256 |
| Mistral-7B | OLMo-7B | 0.56 | 0.56 | 0.00 | 0.720 | 0.725 | 0.584 | 0.605 | 4.333 | 5.778 | 1.472 | 4.222 |
| <i>Cross-family asymmetric</i> | | | | | | | | | | | | |
| Gemma-270M | Qwen-7B | 0.24 | 0.72 | 0.48 | 0.511 | 0.515 | 0.827 | 0.612 | 0.499 | 0.499 | 0.672 | 0.538 |
| Gemma-270M | Llama-3-8B | 0.24 | 0.62 | 0.37 | 0.511 | 0.515 | 0.714 | 0.599 | 0.501 | 0.495 | 0.652 | 0.521 |
| Llama-1B | Qwen-7B | 0.43 | 0.72 | 0.29 | 0.656 | 0.655 | 0.786 | 0.638 | 0.571 | 0.595 | 0.803 | 0.565 |
| Qwen-0.5B | Llama-3-8B | 0.42 | 0.62 | 0.19 | 0.591 | 0.557 | 0.747 | 0.642 | 0.541 | 0.523 | 0.739 | 0.476 |
| Gemma-270M | Llama-1B | 0.24 | 0.43 | 0.19 | 0.511 | 0.515 | 0.566 | 0.538 | 0.496 | 0.509 | 0.623 | 0.422 |
| Gemma-270M | Qwen-0.5B | 0.24 | 0.42 | 0.18 | 0.511 | 0.515 | 0.570 | 0.532 | 0.515 | 0.488 | 0.680 | 0.439 |
| Qwen-0.5B | Llama-1B | 0.42 | 0.43 | 0.01 | 0.591 | 0.557 | 0.580 | 0.605 | 1.267 | 1.294 | 1.811 | 0.344 |
| <i>Same-family asymmetric</i> | | | | | | | | | | | | |
| Qwen-0.5B | Qwen-7B | 0.42 | 0.72 | 0.30 | 0.591 | 0.557 | 0.842 | 0.587 | 0.522 | 0.502 | 0.789 | 0.500 |
| Llama-1B | Llama-3-8B | 0.43 | 0.62 | 0.18 | 0.656 | 0.655 | 0.815 | 0.679 | 0.563 | 0.603 | 0.871 | 0.542 |
| <i>Mean</i> | | | | | 0.596 | 0.606 | 0.727 | 0.627 | 0.848 | 0.972 | 0.915 | 0.741 |

Table 3: Full results on TriviaQA. Pairs grouped by type and sorted by capability gap (descending). **Bold** = best per row among G-Ent, G-PPL, CMP, CME.

| Generator | Verifier | Acc _g | Acc _v | Gap | AUROC ↑ | | | | APGR ↑ | | | |
|--------------------------------|------------|------------------|------------------|------|--------------|--------------|--------------|--------------|--------------|--------------|--------------|--------------|
| | | | | | G-Ent | G-PPL | CMP | CME | G-Ent | G-PPL | CMP | CME |
| <i>Same-size cross-family</i> | | | | | | | | | | | | |
| Llama-3-8B | Qwen-7B | 0.43 | 0.65 | 0.21 | 0.858 | 0.887 | 0.777 | 0.875 | 0.789 | 0.812 | 0.806 | 0.755 |
| Llama-3-8B | Mistral-7B | 0.43 | 0.64 | 0.20 | 0.858 | 0.887 | 0.833 | 0.923 | 0.818 | 0.838 | 0.858 | 0.785 |
| OLMo-7B | Qwen-7B | 0.51 | 0.65 | 0.13 | 0.636 | 0.429 | 0.466 | 0.844 | 0.621 | 0.434 | 0.493 | 0.725 |
| OLMo-7B | Mistral-7B | 0.51 | 0.64 | 0.12 | 0.636 | 0.429 | 0.588 | 0.884 | 0.658 | 0.403 | 0.623 | 0.725 |
| Llama-3-8B | OLMo-7B | 0.43 | 0.51 | 0.08 | 0.858 | 0.887 | 0.611 | 0.822 | 1.068 | 1.119 | 0.774 | 1.071 |
| Mistral-7B | Qwen-7B | 0.64 | 0.65 | 0.01 | 0.848 | 0.300 | 0.420 | 0.766 | 2.222 | -1.068 | -0.562 | 0.093 |
| <i>Cross-family asymmetric</i> | | | | | | | | | | | | |
| Gemma-270M | Qwen-7B | 0.22 | 0.65 | 0.42 | 0.605 | 0.595 | 0.771 | 0.678 | 0.522 | 0.523 | 0.631 | 0.490 |
| Gemma-270M | Llama-1B | 0.22 | 0.54 | 0.32 | 0.605 | 0.595 | 0.686 | 0.683 | 0.509 | 0.509 | 0.596 | 0.444 |
| Gemma-270M | Llama-3-8B | 0.22 | 0.43 | 0.21 | 0.605 | 0.595 | 0.766 | 0.625 | 0.522 | 0.529 | 0.665 | 0.465 |
| Gemma-270M | Qwen-0.5B | 0.22 | 0.41 | 0.18 | 0.605 | 0.595 | 0.650 | 0.601 | 0.482 | 0.491 | 0.596 | 0.368 |
| Qwen-0.5B | Llama-1B | 0.41 | 0.54 | 0.14 | 0.773 | 0.726 | 0.522 | 0.557 | 0.628 | 0.623 | 0.520 | 0.417 |
| Llama-1B | Qwen-7B | 0.54 | 0.65 | 0.10 | 0.805 | 0.811 | 0.691 | 0.788 | 0.696 | 0.724 | 0.764 | 0.574 |
| Qwen-0.5B | Llama-3-8B | 0.41 | 0.43 | 0.03 | 0.773 | 0.726 | 0.619 | 0.525 | 1.403 | 1.264 | 1.337 | 0.472 |
| <i>Same-family asymmetric</i> | | | | | | | | | | | | |
| Qwen-0.5B | Qwen-7B | 0.41 | 0.65 | 0.24 | 0.773 | 0.726 | 0.818 | 0.824 | 0.619 | 0.598 | 0.737 | 0.606 |
| <i>Mean</i> | | | | | 0.731 | 0.656 | 0.658 | 0.742 | 0.825 | 0.557 | 0.631 | 0.571 |

Table 4: Full results on TriviaQA (no ctx). Pairs grouped by type and sorted by capability gap (descending). **Bold** = best per row among G-Ent, G-PPL, CMP, CME.

| Generator | Verifier | Acc _g | Acc _v | Gap | AUROC \uparrow | | | | APGR \uparrow | | | |
|--------------------------------|------------|------------------|------------------|------|------------------|--------------|--------------|--------------|-----------------|--------|--------------|-------|
| | | | | | G-Ent | G-PPL | CMP | CME | G-Ent | G-PPL | CMP | CME |
| <i>Same-size cross-family</i> | | | | | | | | | | | | |
| OLMo-7B | Llama-3-8B | 0.39 | 0.67 | 0.29 | 0.774 | 0.504 | 0.706 | 0.807 | 0.664 | 0.483 | 0.626 | 0.599 |
| OLMo-7B | Mistral-7B | 0.39 | 0.66 | 0.28 | 0.774 | 0.504 | 0.812 | 0.884 | 0.659 | 0.488 | 0.726 | 0.634 |
| OLMo-7B | Qwen-7B | 0.39 | 0.59 | 0.21 | 0.774 | 0.504 | 0.673 | 0.849 | 0.635 | 0.481 | 0.614 | 0.599 |
| Qwen-7B | Llama-3-8B | 0.59 | 0.67 | 0.08 | 0.823 | 0.794 | 0.752 | 0.634 | 0.993 | 0.953 | 0.976 | 0.564 |
| Qwen-7B | Llama-3-8B | 0.59 | 0.67 | 0.08 | 0.823 | 0.794 | 0.752 | 0.634 | 0.993 | 0.953 | 0.976 | 0.564 |
| Qwen-7B | Mistral-7B | 0.59 | 0.66 | 0.07 | 0.823 | 0.794 | 0.712 | 0.682 | 0.877 | 0.843 | 0.869 | 0.596 |
| Qwen-7B | Mistral-7B | 0.59 | 0.66 | 0.07 | 0.823 | 0.794 | 0.712 | 0.682 | 0.877 | 0.843 | 0.869 | 0.596 |
| Mistral-7B | Llama-3-8B | 0.66 | 0.67 | 0.01 | 0.852 | 0.485 | 0.598 | 0.746 | 3.800 | -0.607 | 0.859 | 0.400 |
| <i>Cross-family asymmetric</i> | | | | | | | | | | | | |
| Gemma-270M | Llama-3-8B | 0.10 | 0.67 | 0.57 | 0.700 | 0.666 | 0.828 | 0.696 | 0.524 | 0.525 | 0.570 | 0.470 |
| Gemma-270M | Qwen-7B | 0.10 | 0.59 | 0.49 | 0.700 | 0.666 | 0.792 | 0.680 | 0.499 | 0.503 | 0.591 | 0.416 |
| Qwen-0.5B | Llama-3-8B | 0.21 | 0.67 | 0.46 | 0.791 | 0.786 | 0.772 | 0.576 | 0.561 | 0.560 | 0.614 | 0.495 |
| Qwen-0.5B | Llama-3-8B | 0.21 | 0.67 | 0.46 | 0.791 | 0.786 | 0.772 | 0.576 | 0.561 | 0.560 | 0.614 | 0.495 |
| Gemma-270M | Llama-1B | 0.10 | 0.42 | 0.32 | 0.700 | 0.666 | 0.764 | 0.737 | 0.486 | 0.502 | 0.573 | 0.372 |
| Qwen-0.5B | Llama-1B | 0.21 | 0.42 | 0.21 | 0.791 | 0.786 | 0.613 | 0.647 | 0.529 | 0.525 | 0.585 | 0.426 |
| Qwen-0.5B | Llama-1B | 0.21 | 0.42 | 0.21 | 0.791 | 0.786 | 0.613 | 0.647 | 0.529 | 0.525 | 0.585 | 0.426 |
| Llama-1B | Qwen-7B | 0.42 | 0.59 | 0.17 | 0.840 | 0.851 | 0.738 | 0.806 | 0.655 | 0.675 | 0.758 | 0.506 |
| Gemma-270M | Qwen-0.5B | 0.10 | 0.21 | 0.11 | 0.700 | 0.666 | 0.731 | 0.681 | 0.485 | 0.522 | 0.551 | 0.281 |
| <i>Same-family asymmetric</i> | | | | | | | | | | | | |
| Qwen-0.5B | Qwen-7B | 0.21 | 0.59 | 0.38 | 0.791 | 0.786 | 0.799 | 0.827 | 0.533 | 0.536 | 0.645 | 0.514 |
| Qwen-0.5B | Qwen-7B | 0.21 | 0.59 | 0.38 | 0.791 | 0.786 | 0.799 | 0.827 | 0.533 | 0.536 | 0.645 | 0.514 |
| Llama-1B | Llama-3-8B | 0.42 | 0.67 | 0.25 | 0.840 | 0.851 | 0.938 | 0.813 | 0.687 | 0.694 | 0.813 | 0.588 |
| <i>Mean</i> | | | | | 0.785 | 0.713 | 0.744 | 0.722 | 0.804 | 0.555 | 0.703 | 0.503 |

Table 5: Full results on GSM8K. Pairs grouped by type and sorted by capability gap (descending). **Bold** = best per row among G-Ent, G-PPL, CMP, CME.

| Generator | Verifier | Acc _g | Acc _v | Gap | AUROC \uparrow | | | | APGR \uparrow | | | |
|--------------------------------|------------|------------------|------------------|------|------------------|--------------|--------------|--------------|-----------------|--------------|--------------|--------------|
| | | | | | G-Ent | G-PPL | CMP | CME | G-Ent | G-PPL | CMP | CME |
| <i>Same-size cross-family</i> | | | | | | | | | | | | |
| Mistral-7B | Qwen-7B | 0.51 | 0.90 | 0.39 | 0.655 | 0.539 | 0.668 | 0.729 | 0.575 | 0.513 | 0.590 | 0.619 |
| Mistral-7B | OLMo-7B | 0.51 | 0.83 | 0.32 | 0.655 | 0.539 | 0.705 | 0.699 | 0.565 | 0.507 | 0.610 | 0.584 |
| Llama-3-8B | Qwen-7B | 0.61 | 0.90 | 0.28 | 0.596 | 0.577 | 0.590 | 0.480 | 0.551 | 0.538 | 0.614 | 0.456 |
| Llama-3-8B | OLMo-7B | 0.61 | 0.83 | 0.22 | 0.596 | 0.577 | 0.631 | 0.522 | 0.596 | 0.583 | 0.656 | 0.489 |
| Qwen-7B | Llama-3-8B | 0.60 | 0.75 | 0.15 | 0.467 | 0.479 | 0.201 | 0.207 | 0.260 | 0.310 | 0.041 | 0.013 |
| Mistral-7B | Llama-3-8B | 0.51 | 0.61 | 0.11 | 0.655 | 0.539 | 0.719 | 0.687 | 0.872 | 0.638 | 0.998 | 0.887 |
| OLMo-7B | Qwen-7B | 0.83 | 0.90 | 0.07 | 0.763 | 0.538 | 0.748 | 0.808 | 0.960 | 0.657 | 0.956 | 0.950 |
| <i>Cross-family asymmetric</i> | | | | | | | | | | | | |
| Llama-1B | Qwen-7B | 0.38 | 0.90 | 0.51 | 0.543 | 0.523 | 0.668 | 0.666 | 0.511 | 0.503 | 0.574 | 0.562 |
| Qwen-0.5B | Llama-3-8B | 0.25 | 0.61 | 0.36 | 0.616 | 0.621 | 0.627 | 0.622 | 0.544 | 0.545 | 0.530 | 0.527 |
| Qwen-0.5B | Llama-1B | 0.25 | 0.38 | 0.13 | 0.616 | 0.621 | 0.574 | 0.581 | 0.651 | 0.662 | 0.643 | 0.626 |
| <i>Same-family asymmetric</i> | | | | | | | | | | | | |
| Qwen-0.5B | Qwen-7B | 0.25 | 0.90 | 0.64 | 0.616 | 0.621 | 0.629 | 0.682 | 0.520 | 0.521 | 0.528 | 0.539 |
| Llama-1B | Llama-3-8B | 0.38 | 0.61 | 0.23 | 0.543 | 0.523 | 0.655 | 0.606 | 0.521 | 0.505 | 0.662 | 0.585 |
| <i>Mean</i> | | | | | 0.597 | 0.559 | 0.617 | 0.607 | 0.598 | 0.539 | 0.617 | 0.571 |

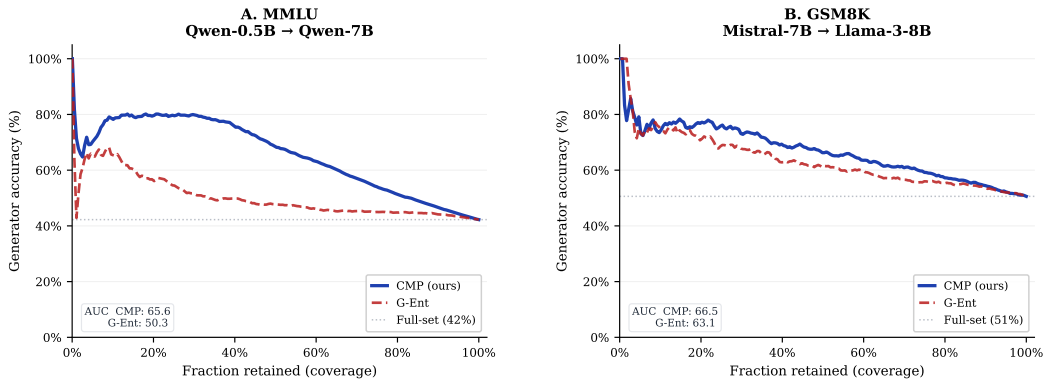


Figure 5: **Coverage–accuracy curves (single pair)**. At each coverage level we abstain on instances whose signal score exceeds a swept threshold and report generator accuracy on the retained subset. CMP (blue, solid) maintains higher accuracy than G-Ent (red, dashed) across nearly all operating points on both MMLU (Qwen-0.5B → Qwen-7B) and GSM8K (Mistral-7B → Llama-3-8B). The dotted line marks full-set accuracy.

A.1 Selective Prediction Analysis

The aggregate metrics in Section 4 (AUROC, APGR, quintile spread) summarise each signal’s ability to rank instances by expected correctness. A complementary perspective comes from *selective prediction* (Geifman & El-Yaniv, 2017), which asks: if we are allowed to abstain on a fraction of inputs, how accurate can we be on the remainder?

We construct coverage–accuracy curves by sweeping an abstention threshold on each signal score. At each threshold we retain only the instances on which the signal is most confident (lowest score) and compute generator accuracy on that retained subset. A stronger signal produces a curve that lies higher: it achieves greater accuracy at the same coverage, or equivalently reaches a target accuracy while retaining more examples.

Single-pair examples. Figure 5 shows curves for two representative pairs (the same ones featured in the quintile figure): Qwen-0.5B → Qwen-7B on MMLU and Mistral-7B → Llama-3-8B on GSM8K. On MMLU, CMP dominates G-Ent across nearly the full coverage range; at 20% coverage the most confident CMP predictions approach perfect accuracy, whereas G-Ent remains closer to the full-set baseline. On GSM8K the two curves are closer together, but CMP maintains a consistent advantage, particularly at low coverage.

Aggregate trends. To verify that these patterns are not pair-specific, Figure 6 averages the coverage–accuracy curves across all 15 model pairs per benchmark (shaded bands show ± 1 standard error). The averaged curves confirm the single-pair findings: CMP lies above G-Ent at virtually every operating point on both MMLU (AUC 60.4 vs. 53.1) and GSM8K (AUC 42.5 vs. 40.3). These AUC summaries are consistent with the AUROC and quintile-spread rankings in Section 4, and confirm that the advantage of cross-model perplexity extends to the operationally relevant setting where a system must decide, per query, whether to serve a generation or abstain. This makes CMP directly applicable as an abstention trigger in high-stakes settings where a confident wrong answer is costlier than no answer.

B Effect of Capability Gap

Figures 7 and 8 provide additional context for the capability gap by including within-model entropy as a comparison signal. Figure 7 plots both CMP and entropy AUROC on the same axes, showing that the positive gap effect on TriviaQA is specific to CMP — entropy shows no significant correlation with gap on any dataset. Figure 8 plots the difference directly ($\Delta\text{AUROC} = \text{CMP} - \text{G-Ent}$), confirming that CMP’s advantage over entropy grows with capability gap on TriviaQA ($\rho = +0.75, p < 0.01$) but not on MMLU or GSM8K.

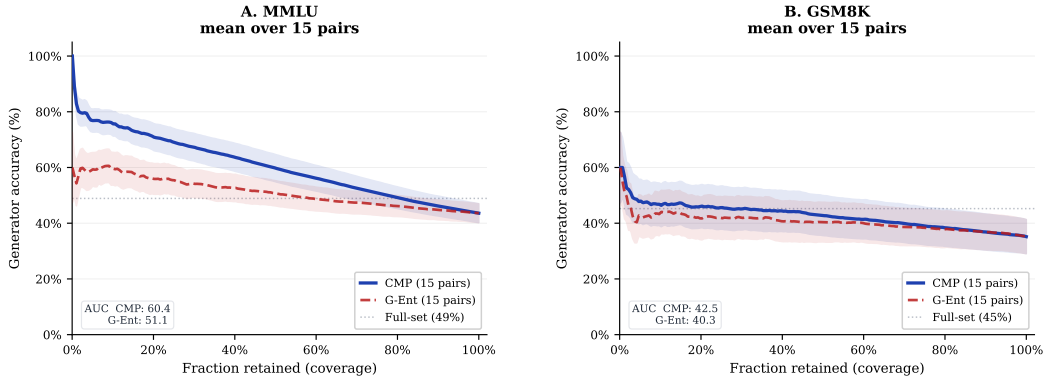


Figure 6: Coverage-accuracy curves (averaged over all pairs). Curves are averaged across all 15 model pairs per benchmark; shaded bands show ± 1 SE. CMP consistently achieves higher accuracy than G-Ent at equal coverage on both MMLU and GSM8K.

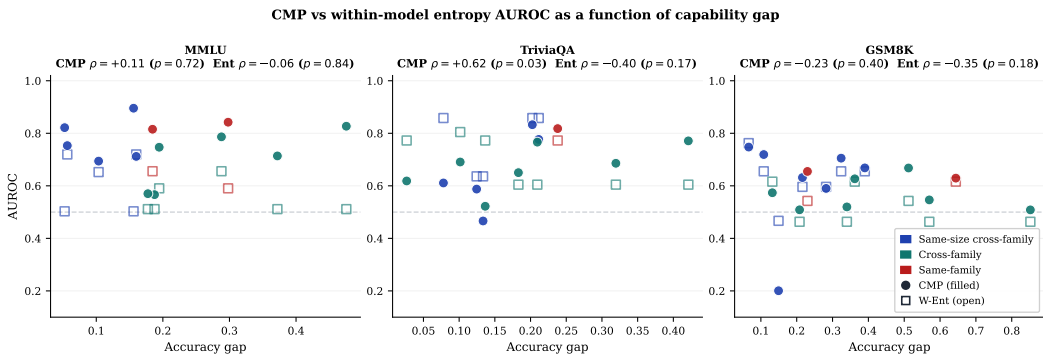


Figure 7: CMP (filled circles) and within-model entropy (open squares) AUROC versus capability gap. The positive gap effect on TriviaQA is specific to CMP — entropy AUROC is uncorrelated with gap on all three datasets.

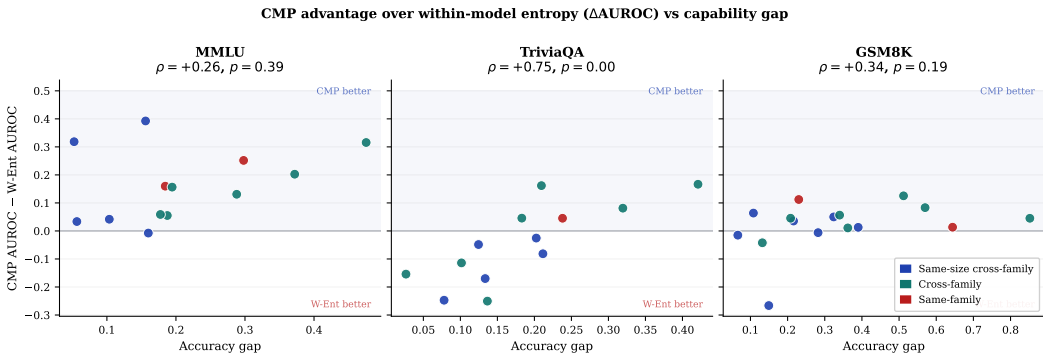


Figure 8: CMP advantage over within-model entropy ($\Delta\text{AUROC} = \text{CMP} - \text{G-Ent}$) versus capability gap. CMP’s advantage grows significantly with gap on TriviaQA ($\rho = +0.75$, $p < 0.01$), while on MMLU CMP leads regardless of gap size. GSM8K shows a positive but non-significant trend ($\rho = +0.34$, $p = 0.19$).

C Experimental Setup Details

Models. We evaluate across a diverse set of model pairs spanning multiple families and capability levels. Generating models include Qwen2.5-0.5B-Instruct, Qwen2.5-1.5B-Instruct, Llama-3.2-1B-Instruct, Llama-3.2-3B-Instruct, gemma-3-270m-it, and SmolLM2-1.7B-Instruct. Verifying models include Qwen2.5-7B-Instruct and Meta-Llama-3-8B-Instruct. We additionally evaluate *same-sized cross-family* pairs—models with comparable parameter counts but different architectures and training corpora, including Mistral-7B-Instruct-v0.3, OLMo-3-7B-Instruct, and Meta-Llama-3-8B-Instruct as both generators and verifiers—to isolate the effect of model diversity from capability asymmetry.

Datasets. We evaluate on four benchmarks spanning distinct task types. **MMLU** (Hendrycks et al., 2021) is a 57-subject multiple-choice benchmark testing knowledge and reasoning; we use single-token answer generation. **TriviaQA** (Joshi et al., 2017) is evaluated in both the no-context variant, testing pure knowledge retrieval, and the context variant, testing reading comprehension. **GSM8K** (Cobbe et al., 2021) requires multi-step chain-of-thought reasoning, with answers evaluated by extracting the final numerical value. We evaluate on up to 2000 examples per dataset with a fixed random seed.

Implementation. All models are loaded in bfloat16 precision. Generations use greedy decoding with maximum token lengths of 5 (MMLU), 8 (TriviaQA), and 256 (GSM8K). The verifying model performs only a single prefill forward pass and never generates tokens. All experiments are run on a single NVIDIA A10G GPU (24GB).

D Relationship to Generation-Based Correctness Signals

The baselines in our main experiments—generator entropy (G-Ent) and generator perplexity (G-PPL)—are chosen as direct ablations of the cross-model design decision: they answer whether the verifying model’s distribution adds signal over the generating model’s own distribution, holding the computational regime constant. This appendix clarifies how CMP and CME relate to generation-based correctness signals that occupy a different point on the compute-accuracy tradeoff.

D.1 Consistency-Based Methods

SelfCheckGPT (Manakul et al., 2023) and CrossCheckGPT (Sun et al., 2024) detect errors by measuring consistency across multiple stochastic samples from the same model or across outputs from independent models. These methods can achieve strong hallucination detection performance, but operate in a fundamentally different compute regime: they require k full autoregressive generation passes, where k is typically 3–5, compared to the single prefill forward pass required by CMP and CME. For answer lengths typical of our benchmarks (up to 256 tokens for GSM8K) this represents a substantial difference in inference cost.

Beyond compute, consistency-based methods are conceptually distinct from cross-model disagreement. SelfCheckGPT measures whether a model agrees with itself across samples; CMP measures whether a second model is surprised by the generating model’s specific answer. The two signals are complementary: consistency captures within-model variance, while CMP captures between-model disagreement on a fixed output. CMP could in principle be extended to sampled rather than greedy answers—computing mean verifier perplexity over k samples—which would interpolate between the two approaches and may improve signal quality at higher compute cost. We leave this extension to future work.

We do not claim that CMP outperforms consistency-based methods unconditionally. Rather, CMP occupies the low-cost end of the correctness signal spectrum: it provides a meaningful signal with no labeled data, no generation from the verifier, and no repeated sampling from the generator. This makes it most attractive in latency-constrained or cost-constrained deployment settings where multiple generation passes are not feasible.

D.2 Generation-Based Judge Methods

A related line of work uses a language model as a judge to evaluate another model’s outputs (Zheng et al., 2023; Kim et al., 2024; Dubois et al., 2024). These approaches require the judge model to *generate* a response—typically a scalar rating or structured critique—which is one to two orders of magnitude more expensive than a prefill pass. They also target output quality and preference rather than per-instance binary correctness, making direct AUROC comparison inappropriate. Self-evaluation methods such as P(True) (Kadavath et al., 2022) similarly require generation from the evaluating model and are known to be unreliable on smaller models, which constitute most of our generator set.

CMP and CME differ from all of these in that the verifying model never generates tokens: it performs only a prefill pass and produces a scalar signal directly from its output logits. This constraint is what enables the single-forward-pass efficiency claim, and it is what distinguishes our contribution from the LLM-as-Judge literature.

D.3 Why G-Ent and G-PPL Are the Appropriate Ablations

Given the above, G-Ent and G-PPL are the correct ablation baselines for our research question. The central claim of this paper is that a verifying model’s distribution over a generating model’s answer contains correctness signal beyond what is already present in the generating model’s own distribution. G-Ent and G-PPL isolate exactly this question: they are the within-model analogues of CME and CMP respectively, computed from the same answer under the same greedy decoding setting, with no verifier involved. Any performance gap between CMP and G-PPL, or between CME and G-Ent, is attributable solely to the cross-model signal. Comparing against generation-based methods would conflate this signal with sampling variance, generation length, or judge calibration, obscuring the contribution we seek to measure.

E Failure Mode: Very Weak Generators on Reasoning Tasks

CMP requires the generator to produce a meaningful mixture of correct and incorrect answers. On knowledge tasks (MMLU, TriviaQA), even Gemma-3-270M at 10–24% accuracy provides enough signal for CMP to achieve AUROC 0.57–0.83. However, on GSM8K where Gemma-3-270M achieves only 4% accuracy, CMP collapses to near-random (Table 6). At this accuracy level, virtually all generated answers are incorrect chain-of-thought reasoning with wrong final numbers, leaving the verifier no distributional contrast to exploit. We observe that CMP degrades gracefully: the threshold for useful signal is approximately 10% generator accuracy, below which both CMP and generator-entropy baselines become uninformative.

Table 6: GSM8K results with Gemma-3-270M as generator (4% accuracy). All routing signals collapse to near-random when the generator almost never produces correct answers.

| Verifier | Acc _v | Gap | AUROC ↑ | | APGR ↑ | |
|-------------|------------------|------|---------|-------|--------|-------|
| | | | G-Ent | CMP | G-Ent | CMP |
| Qwen-7B | 0.90 | 0.85 | 0.463 | 0.508 | 0.500 | 0.508 |
| Llama-3-8B | 0.61 | 0.57 | 0.463 | 0.546 | 0.476 | 0.487 |
| Llama-1B | 0.38 | 0.34 | 0.463 | 0.520 | 0.506 | 0.533 |
| Qwen-0.5B | 0.25 | 0.21 | 0.463 | 0.509 | 0.453 | 0.489 |
| <i>Mean</i> | | | 0.463 | 0.521 | 0.484 | 0.504 |

F GSM8K: Final-Answer Tokens and Verification Prompting

The chain-of-thought sequences in GSM8K raise a natural question: does the routing signal come from the full reasoning trace or only the final numerical answer? We additionally test whether an explicit verification prompt—asking the verifier “Is this answer correct?”—can match or exceed the implicit signal in CMP.

Final-answer CMP. We extract the token positions corresponding to the final numerical answer (the digits after the ANSWER: marker) and compute CMP restricted to those positions

Table 7: GSM8K correctness prediction (AUROC): Full chain-of-thought CMP vs. final-answer-only CMP vs. P(True) verification prompting. CMP-Full and CMP-Final perform comparably, while P(True) is near random. **Bold** = best among CMP-Full, CMP-Final, P(True).

| Generator | Verifier | Acc _g | Gap | AUROC \uparrow | | | Baselines | |
|-------------|------------|------------------|------|------------------|--------------|---------|-----------|-------|
| | | | | CMP-Full | CMP-Final | P(True) | G-Ent | G-PPL |
| Qwen-0.5B | Qwen-7B | 0.25 | 0.64 | 0.629 | 0.456 | 0.495 | 0.616 | 0.621 |
| Llama-1B | Qwen-7B | 0.38 | 0.51 | 0.668 | 0.755 | 0.463 | 0.543 | 0.523 |
| Mistral-7B | Qwen-7B | 0.51 | 0.39 | 0.668 | 0.574 | 0.487 | 0.655 | 0.539 |
| Qwen-0.5B | Llama-3-8B | 0.25 | 0.36 | 0.627 | 0.525 | 0.431 | 0.616 | 0.621 |
| Llama-3-8B | Qwen-7B | 0.61 | 0.28 | 0.590 | 0.584 | 0.476 | 0.596 | 0.577 |
| Llama-1B | Llama-3-8B | 0.38 | 0.23 | 0.655 | 0.611 | 0.417 | 0.543 | 0.523 |
| Mistral-7B | Llama-3-8B | 0.51 | 0.11 | 0.719 | 0.583 | 0.436 | 0.655 | 0.539 |
| OLMo-7B | Qwen-7B | 0.83 | 0.07 | 0.748 | 0.854 | 0.497 | 0.763 | 0.538 |
| <i>Mean</i> | | | | 0.663 | 0.618 | 0.463 | 0.623 | 0.560 |

only (CMP-Final), compared to CMP over the full chain-of-thought (CMP-Full). Across 8 model pairs (Table 7), CMP-Final achieves mean AUROC of 0.618 versus 0.663 for CMP-Full and mean APGR of 0.665 versus 0.682 (Table 8). On most pairs CMP-Full leads, but CMP-Final matches or exceeds it on two pairs (Llama-1B \rightarrow Qwen-7B and OLMo-7B \rightarrow Qwen-7B), suggesting that the verifier’s disagreement signal is largely concentrated in the final answer rather than distributed across intermediate reasoning steps. This implies CMP could be applied more efficiently by scoring only the answer tokens, avoiding the cost of processing the full chain-of-thought through the verifier.

Verification prompting. We test an explicit P(True) baseline (Kadavath et al., 2022): we prompt the verifier with the question and the generator’s proposed answer, asking “Is the proposed answer correct? Yes or No,” and extract the probability assigned to the “Yes” token. Despite being a natural approach to answer verification, P(True) achieves mean AUROC of only 0.463—below random (0.504)—and mean APGR of 0.492. The verifier’s explicit judgment of correctness is far less informative than its implicit token-level perplexity on the same answer. This is consistent with known limitations of LLM self-evaluation on mathematical reasoning: models that cannot reliably solve a problem also cannot reliably judge whether a solution is correct when asked directly.

Table 8: GSM8K routing performance (APGR): Full chain-of-thought CMP vs. final-answer-only CMP vs. P(True). Pairs with gap < 5pp excluded. **Bold** = best among CMP-Full, CMP-Final, P(True).

| Generator | Verifier | Acc _g | Gap | APGR \uparrow | | | Baselines | |
|-------------|------------|------------------|------|-----------------|--------------|---------|-----------|-------|
| | | | | CMP-Full | CMP-Final | P(True) | G-Ent | G-PPL |
| Qwen-0.5B | Qwen-7B | 0.25 | 0.64 | 0.528 | 0.484 | 0.499 | 0.520 | 0.521 |
| Llama-1B | Qwen-7B | 0.38 | 0.51 | 0.574 | 0.621 | 0.481 | 0.511 | 0.503 |
| Mistral-7B | Qwen-7B | 0.51 | 0.39 | 0.590 | 0.524 | 0.506 | 0.575 | 0.513 |
| Qwen-0.5B | Llama-3-8B | 0.25 | 0.36 | 0.530 | 0.509 | 0.492 | 0.544 | 0.545 |
| Llama-3-8B | Qwen-7B | 0.61 | 0.28 | 0.614 | 0.579 | 0.488 | 0.551 | 0.538 |
| Llama-1B | Llama-3-8B | 0.38 | 0.23 | 0.662 | 0.636 | 0.463 | 0.521 | 0.505 |
| Mistral-7B | Llama-3-8B | 0.51 | 0.11 | 0.998 | 0.967 | 0.483 | 0.872 | 0.638 |
| OLMo-7B | Qwen-7B | 0.83 | 0.07 | 0.956 | 1.000 | 0.525 | 0.960 | 0.657 |
| <i>Mean</i> | | | | 0.682 | 0.665 | 0.492 | 0.632 | 0.552 |